IEEE Access
Multidisciplinary | Rapid Review | Open Access Journal

Received July 1, 2017, accepted July 13, 2017, date of publication July 18, 2017, date of current version August 8, 2017.

Digital Object Identifier 10.1109/ACCESS.2017.2728623

Energy and Congestion-Aware Routing Metric for Smart Grid AMI Networks in Smart City

REHMAT ULLAH[1], YASIR FAHEEM[2], AND BYUNG-SEO KIM[3], (Member, IEEE)

[1]Department of Electronics and Computer Engineering, Hongik University, Sejong 30016, South Korea
[2]Department of Computer Science, COMSATS Institute of Information Technology, Islamabad 45550, Pakistan
[3]Department of Computer and Information Communications Engineering, Hongik University, Sejong 30016, South Korea

Corresponding author: Byung-Seo Kim (jsnbs@hongik.ac.kr)

This work was supported by the Basic Science Research Program through the National Research Foundation of Korea from the Ministry of Education under Grant 2015R1D1A1A01059186.

ABSTRACT Advanced metering infrastructure (AMI) is becoming a vital part of utility distribution networks, allowing the development of smart cities. AMI consists of smart electric, gas, and water meters, and the devices are very limited in terms of battery, processing power, and memory. The deployment and operational needs of energy-constrained network infrastructures in smart water and gas metering systems require the use of routing mechanisms that consider energy consumption, minimize energy use, and prolong network lifetime. An efficient routing metric is needed for energy-constrained devices. In this paper, we propose an energy- and congestion-aware routing metric for smart meter networks to be deployed in smart cities. The proposed metric is an adaptive parent node selection mechanism that considers the residual energy and queue utilization of neighboring nodes. Minimizing power consumption will enhance network lifetime. The proposed scheme was evaluated with the Cooja Simulator 3.0 using random and grid topology. The simulation results show greater network performance in terms of average power consumption and packet delivery ratio.

INDEX TERMS Low power and lossy networks, smart city, smart grid, 802.15.4, advance metering infrastructure (AMI), IoT, 6LoWPAN.

I. INTRODUCTION

The smart grid [1] is a new concept related to the legacy power grid. In basic terms, it consists of a network that integrates communication technology with electric power infrastructures. This architecture can significantly improve the robustness and efficiency of the generation, transmission, and distribution of electrical systems. A smart grid plays an important role in a smart city by modernizing power systems, efficient energy usage, and providing reliable integration of distributed and renewable energy resources. These roles make smart grids invaluable for the smart cities. AMI is a fundamental component of the smart grid, allowing two-way communication between electric, gas, and water meters and city utility companies [2]. A smart meter is the basic component of a smart grid AMI Networks. A smart city uses digital technology to improve the overall productivity, optimize the usage of resources like: Electricity, Gas and Water. The same idea of AMI can be extended to other common utilities like gas and water. In utilities of water and gas, the meters acts as leaf nodes in a sensor network, that collect and forward measurements to an aggregator unit [3]. In the smart cities, extensive data will flow from many sources, which will be carry out over many communication networks to be analyzed, and integrated for providing benefit to all in smart cities. AMI are becoming a vital part of the water, electric, and gas utility distribution networks, enabling the measurement, configuration, and control of energy, gas, and water consumption through two-way scheduled and on-demand communication [4]. AMI networks are composed of millions of endpoints, including smart meters, distribution automation elements, and, eventually, home area network (HAN) devices. They are typically interconnected using some combination of wireless and power-line communications [5].

Utility companies have considered both wired and wireless communication technologies for building AMI networks. Wired technologies are considered superior to wireless technologies, in terms of reliability, security, and bandwidth, because cables are easier to protect from interference and eavesdroppers. Furthermore, wired equipment is generally cheaper than wireless. On the other hand, wireless networks offer low installation costs and enable rapid deployment, even over large areas. Recent advances in broadband wireless

technologies provide data rates and network capacities comparable to those of popular wired networks. For these reasons, it is commonly accepted by utility companies that increasing portions of their AMI systems can rely on wireless communication technologies [6].

Typical smart meters are resource-constrained, embedded devices with limited processing power and storage capabilities. In AMI networks, links between devices are generally characterized by the high packet loss rates, low bandwidth, and instability due to unplanned network deployments and the use of low-power link layer technologies, such as IEEE 802.15.4g, IEEE 802.15.4e, IEEE 1901.2, and IEEE 802.11 standards [7]. These types of networks are typically referred to as low-power and lossy networks (LLNs). In recent years, several routing protocols have been proposed for this network category [8]; however, the most mature and commercially viable solution is the routing protocol for LLN (RPL) [9], with standardization completed by the Internet Engineering Task Force (IETF) in March 2012. RPL is intended to meet the requirements of a wide range of LLN application domains, including building automation, urban sensor networks, and large-scale AMI systems [10]. RPL is further explained in section II.

In most scenarios, electric meters are powered by the main line of the grid they monitor and, they can afford the additional resources required to route packets [11], [12]; therefore, electric smart meters are beyond the scope of this study. Gas and water meters typically run on a modest source of stored energy (e.g., batteries), so our focus will be on distribution network solutions for smart gas and water meters. We will also provide an overview of the RPL routing protocol, which is emerging as the de facto Internet related routing protocol for AMI applications.

The remainder of this article is organized as follows: Section II explains the RPL in detail; section III introduces motivations and the proposed scheme; performance evaluations are described in section IV; and, finally, section V discusses our conclusions.

II. ROUTING PROTOCOL FOR LLN (RPL)

RPL is a standard routing protocol for LLNs [9]. LLNs consist of up to thousands of embedded sensing devices that are resource-constrained in terms of processing capability, memory, transmission range, and battery life. In LLNs, hundreds to thousands of motes are deployed in the environment, forming a multi-hop network that senses, collects, and relays information to one or several points connected to the Internet [15]. Through the Internet, the data is forwarded to a meter data management system (MDMS), which can be located in the power substation as shown in Fig. 1. MDMS refers to software that performs data storage and management for the large amount of data delivered by smart metering systems.

RPL organizes a network into one or more destination-oriented direct acyclic graphs (DODAGs) [14]. Each DODAG ends at a single point called the root. The root initiates topology construction by sending DODAG information

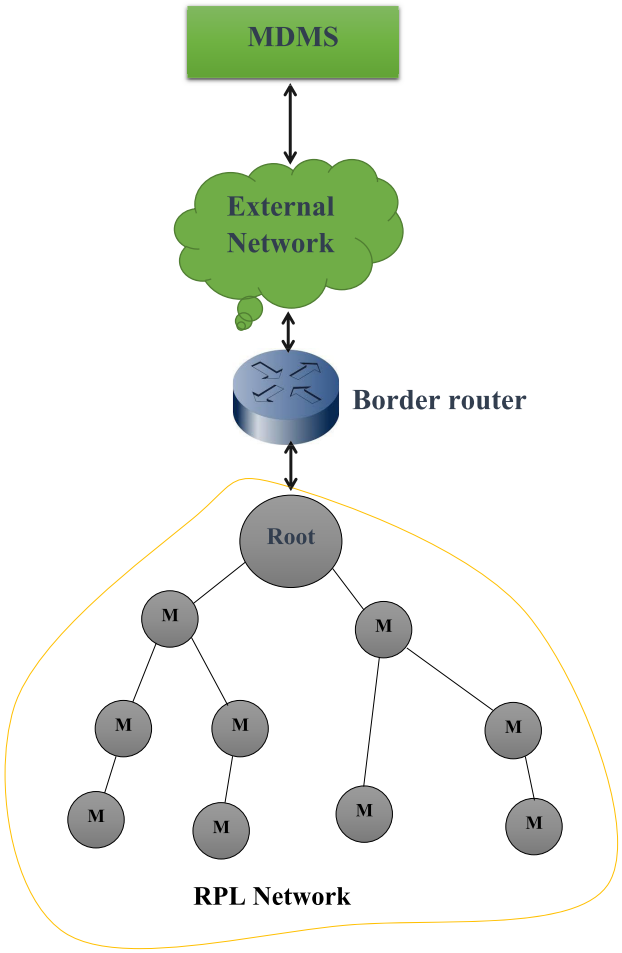

FIGURE 1. Smart meters in RPL network connecting with MDMS via border router and IP Network.

object (DIO) messages periodically to all the nodes within transmission range. DIO messages contain all the important information about the topology construction, such as the unique identity of the root, version number, rank, and other necessary routing metrics [9]. A DIO Packet format [9] is shown in Fig. 2. All nodes in the vicinity, after receiving the DIO messages, joins with the DODAG and select its preferred parent nodes or parent nodes as next hop towards the root.

Parent node selection depends upon the objective function (OF), which uses routing metrics to select the preferred parent node among multiple neighbors. An OF specifies how RPL nodes choose and create optimal paths inside RPL networks. Routing over Low-power and Lossy network (RoLL) working group has specified two OFs, Minimum Rank with Hysteresis Objective Function (MRHOF) [17] and Objective Function Zero (OF0) [18]. RPL uses the MRHOF as a default metric for path calculation. MRHOF selects routes based on Expected Transmission Count (ETX). The main goal of ETX is to choose routes with high end-to-end throughput, which is defined as follows [19]:

$$ETX = \frac{1}{d_f \times d_r} \tag{1}$$

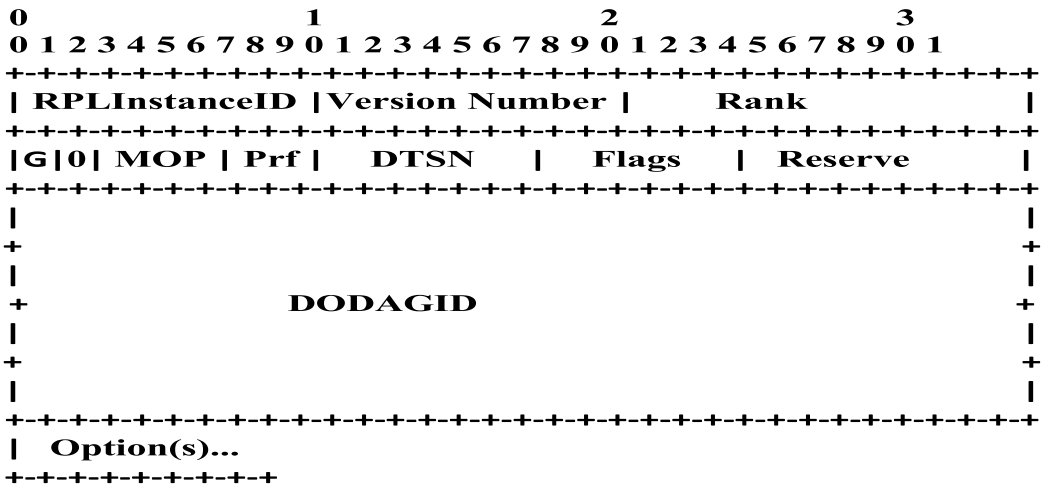

FIGURE 2. RPL DIO packet format.

where d_f represents forward delivery ratio which is the measured probability that a packet is received by a neighbor. The d_r represents reverse delivery ratio which is the probability that an acknowledgment packet is successfully received. The expected probability that a transmission is successfully received and acknowledged is $d_f \times d_r$. A sender will retransmit a packet that is not successfully acknowledged.

The OF0 uses minimum hop count for selecting best parent node. The DODAG construction is based on the rank of a node, which depicts a scalar representation of the location of a node in a DODAG with respect to DODAG root. In order to have a loop free DODAD, the rank must monotonically increase from the root towards the leaves of the DODAG. The rank of root must be minimum in DODAG. Rank of a node, k, is defined as follows [9]:

$$Rank\ (k) = Rank\ (parent) + Rank\_increase \tag{2}$$

where $Rank\_increase = MinHopRankIncrease$ and the standard value of $MinHopRankIncrease$ is 256 [17]. DODAG root provides $MinHopRankIncrease$ for DAG construction. For loop detection or for determination child parent node relationship, the integer portion of the rank is used. The integer portion of the rank can be computed by $DAGRank()$ which is defined as follows:

$$DAGRank\ (Rank) = floor\left(\frac{Rank}{MinHopRankIncrease}\right) \tag{3}$$

where $floor\ (x)$ is the function that looks at to the greatest integer less than or equal to x. Table 1 shows an example of rank calculation.

The design and selection of routing metrics that meets different application's requirement are still an open research issue. Using ETX for selecting the parent node with the best quality link may cause a load-balancing problem. Nodes that are closer to the root may have many children with good-quality links, thus receiving and forwarding a large number of packets, which may quickly deplete the battery.

TABLE 1. An example of rank calculation.

NodeID	Node Rank	Integer Portion
1	256	1
2	512	2
3	768	3
4	1024	4

Ha *et al.* [21] and Liu *et al.* [22] investigated load-balancing problems when using multiple gateways; however, they were only able to reduce traffic congestion by using additional gateways.

Gaddour and Kouba [20] proposed QoS-aware fuzzy logic; however, it is not clear which metric should be optimized for specific applications. Several studies have been done on load balancing in RPL [21], [22].

Recently, Kim *et al.* [15] proposed Queue Utilization RPL (QU-RPL) for load balancing under heavy traffic. QU-RPL takes the queue utilization of neighboring nodes into consideration when selecting parent nodes. The authors further described queue utilization factor (QU) as the number of packets in the queue divided by total queue size. QU factor of each node k can be defined as follows [15]:

$$Q_{(k)} = \frac{N\ (p)}{S\ (q)} \tag{4}$$

where $N\ (p)$ shows the number of packets in the queue and $S\ (q)$ shows the total size of the queue. In QU-RPL, residual energy of nodes is not considered while selecting the preferred parent node. In case the parent node depletes the battery, not only will the packets be lost, but inconsistencies will also emerge throughout the network. The strongest nodes will suffer packet loss due to battery depletion, requiring reconfigurations of the DODAG. As a result load balancing and congestion will be arise in the network. Nassiri *et al.* [16] proposed a load balancing algorithm

"Energy aware and load balancing parent selection in RPL routing for wireless sensor network" (ELPS), which is based on modified cluster-tree Medium Access Control (MAC) protocol. We propose residual-energy and queue congestion-based parent node selection mechanism that will increase lifetime of the network and enhance performance in terms of PDR in AMI networks. For carrying information of ETX, hop-count, QU and Residual energy of nodes, we exploited the conventional DIO packet format according [23].

A conventional DIO RPL Packet format [9] is shown in Fig. 2 and the different fields are described below.

RPLInstanceID: It is an 8-bit field and shows the RPL Instance the DODAG belongs to.

Version Number: It is an 8-bit field and shows the freshness of the DODAG.

Rank: It is a 16-bit field showing the rank of the node sending the DIO.

Grounded: It is a flag and is set when the root of the DODAG is connected to the public Internet.

O: It is set to 0.

Mode of Operation (MOP): It is a 3bit field and indicates one of the four defined modes of operation of RPL (0: No downward routes maintained by RPL, 1: Non-storing mode, 2: Storing without multicast support, 3: Storing with multicast support). The storing mode means the nodes are capable of storing routing information. In non-storing mode, no routing tables are maintained.

DODAG Preference: The default value is 0. It is set by root to report its preference over other DODAG roots in the RPL instance.

Destination Advertisement Trigger Sequence Number (DTSN): It is an 8-bit field set by the node issuing the DIO message. DTSN flag is used as part of the procedure to maintain downward routes.

Flags: It is an 8 bit field reserved for flags, initialized to 0 by sender and ignored by receiver.

Reserved: It is an 8-bit unused field, initialized to 0 by sender and ignored by receiver.

DODAGID: It is 128-bit field which uniquely identifies the DODAG and is set to the IPv6 address of the root.

Options: This field contains implementation specific values. In Contiki it may contains metric container type and flags. In our scheme, we used this field for metric container type of Node state object, Node Energy object, Hop count object and ETX object, which is explained in Section III-C.

III. ENERGY AND CONGESTION-AWARE ROUTING METRIC (ECRM)

In this section, to clarify the features of the proposed scheme, a motivation of this paper is provided. After that, a novel scheme is proposed. In a nut shell, the ultimate goal of the proposed scheme is to enhance network performances in terms of the network's life time and PDR by selecting appropriate parent node which has more residual energy and less queue congestion than others.

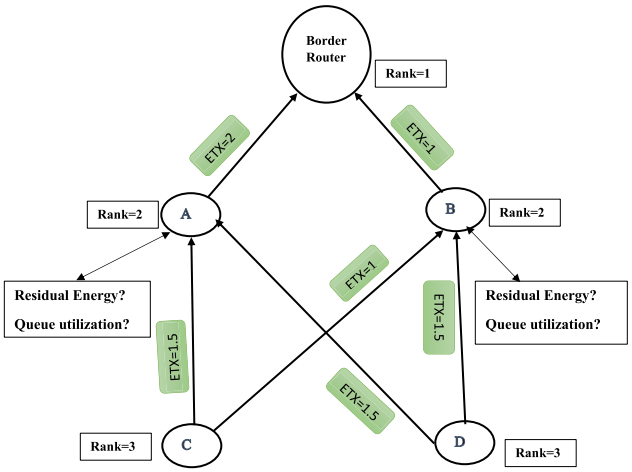

FIGURE 3. An example of DODAG construction and parent node selection.

A. MOTIVATIONS

The motivation might be illustrated by using an example shown in Fig. 3. The figure shows an example of a network configuration and how routing DAG is constructed based on the values of rank and ETX. As shown in Fig. 3, Node C and D have Node A and B as the best parent candidate nodes and eventually, both nodes chooses Node B as the best parent node. Let's assume that Node C chooses Node B as the best parent node at first and then Node D does later. Therefore, eventually, Node C and D transmit their own data or forward their child nodes data to Node B. However, if the residual energy of Node B is much less than that of Node A, the communications between Node C/D and B will be disconnected because of the depletion of Node B's energy. As a result, Node C and D will start over the process to find and to set the best parent node, which causes undesirable network overhead. Instead of choosing Node B, Node A might be the better choice for the best parent node of them. Thus, the network may not trigger local or global repair mechanism for reconfiguration of the topology and as a consequence, the performances of the network would be better. Beside of the residual energy issue, the queue status of the best parent node may effect on the network performances. For instance, since Node B is the parent node of both Node C and D, the queue of Node B might be congested. If more nodes in the network select Node B as their parent node, the queue of Node B is over congested and packets may be dropped due to queue overflow. Therefore, if the other node (in the example, Node A) with less congested queue status were selected as a parent node, the packet drop could have avoided. In summary, as we described above with Fig. 3, in order to improve network performances, the status of the residual energy and queues of the parent candidate nodes need to be considered in order to choose the best parent node. Therefore, the objective of the proposed scheme in this paper is to provide a way to improve the network performances by considering the both factors (residual energy and queue status).

B. PROPOSED SCHEME FORMULATION

Let's consider a LLN system consisting of LLN endpoints or meters rooted at the border router, the architecture of which is shown in Fig. 1. All meters sense, collect, and relay data to their preferred parent node. The LLN is modeled by a direct graph of S (V, E), where V represents the number of vertices or nodes and E represents the edges that connect vertices. Starting from border router, RPL constructs a DAG based on the rank of a node. At the start of network initialization, the border router broadcasts DIO messages contain information such as rank, DODAG's identity, version number and the OF. When nodes receives DIO messages from the border router, a rank is calculated for each node according to Eq. (2) and Eq. (3). According to the integer value of Eq. (3), all the nodes will locate themselves in DODAG. The topology may be constructed in such way that the root node must have minimum rank and all the parent nodes must have minimum rank than their child nodes. When the topology is constructed, then each node will periodically start broadcasting DIO messages. These packets contain information about their rank, QU factor, energy state, ETX value and DODAG's identity. When a node receives DIO messages from neighboring nodes, it generates a parent candidates set of nodes with hop count of 3 hops and minimum ETX of 3 hops to the border router. According to [19], ETX predicts throughput for short routes of 1, 2 or 3 hops. From all the nodes in the candidates set, the node will choose a parent node having residual energy and QU with in a certain level and lowest rank and ETX to the border router. Each node changes its current parent node when information on parent candidates has been changed. In this article, we propose a routing metric, $R_{pro}(p_k)$, for selecting the best alternative parent, which is defined as follows:

$$R_{pro}(p_k) = Rank(p_k) + ETX(k, p_k) + \alpha Q(p_k) + \beta E_{res}(p_k) \tag{5}$$

where $Rank(p_k)$ is the scaler rank value of parent node p_k, $ETX(k, p_k)$ shows the ETX value from node k to parent node p_k. $Q(p_k)$ is the QU on parent node p_k. α is a coefficient which controls the weight given to the QU. $E_{res}(p_k)$ is the residual energy of the parent node p_k and β is the weight given to $E_{res}(p_k)$. α and β are design parameters which is explained in Section VI-A and VI-B. Therefore, the parent node p_k will be changed to the best alternative parent node $\hat{p}_k$ if the following condition is met,

$$E_{res}(p_k) < E_{thresh} \tag{6}$$

The best alternative parent node will be selected if the residual energy of the current parent node is less than the threshold according Eq. (6). If Eq. (6) is not satisfied, Eq. (7) will be checked for congestion, as follows [15]:

$$\mu_k > \gamma \tag{7}$$

where μ_k is the traffic congestion condition indicating traffic congestion around node k, and γ is a threshold value for deciding when to perform parent switching.

Regarding μ_k, Kim *et al.* [15] explained that the QU of parent node $Q(p_k)$ cannot properly reflect traffic congestion. Once the traffic load is well balanced, after satisfying Eq. (7), each node changes its parent node, as in conventional RPL, causing the traffic load to become unbalanced again. Therefore, the authors exploited $Q_{k,\max}$, which is the maximum QU among all parent candidates recently selected by node k, and is defined as follows [15]:

$$Q_{k,\max} = \max\left\{Q_{k,\max}, \max_{p_k \in p_k}\{Q(p_k)\}\right\} \tag{8}$$

Using $Q_{k,\max}$, each node memorizes the previous congestion event, meaning $Q_{k,\max}$ maintains the record of recent congestion events and mitigates problems caused by fast parent changes.

A node will therefore change the current parent node, p_k, to the best alternative node, $\hat{p}_k$, if:

$$\mu(p_k) > \gamma \tag{9}$$

Eq. (9) shows that the best alternative parent will be selected if the congestion of the current parent is greater than the threshold.

First, Eq. (6) is checked to avoid energy-constrained nodes. If the conditions of Eq. (6) and Eq. (7) are not satisfied, this means the residual energy of the candidate parent node is sufficient and there is no congestion as well. Therefore, the node changes its parent node from p_k to $\hat{p}_k$ in the same way as in conventional RPL.

C. PROPOSED SCHEME DESCRIPTION

RPL is a distance vector routing protocol that builds Directed Acyclic Graphs (DAGs) based on routing metrics and constraints. The routing metrics and constraints are advertised in the DIO message specified in [9]. DAG Metric Container object exists in the option field of RPL DIO packet format. Routing metrics or constraints are carried within the DAG Metric Container object defined in [9]. There can be multiple metrics and constraints in the DAG Metric Container. The best path can be defined by an OF [23].

In our propose scheme, we used different metrics and constraints (QU, hop count, ETX and Residual energy). Four object fields are depicted in Fig. 5 for carrying information such as QU, hop count, ETX and Residual energy. The process of propose scheme is shown in Fig. 4 as a flow chart and the detailed description of the process is given as follows:

Step 1. Each node recognize its neighbor nodes by DIO messages received periodically from them including information of rank, ETX, QU and residual energy costs of the nodes.

Step 2. A node generates a parent candidates set from its neighbor nodes. Parent candidates set consist of nodes have hop count of 3 hops and ETX of 3 hops to the border router.

Step 3. Each node performs parent node selection process, when its information on parent candidate has been changes.

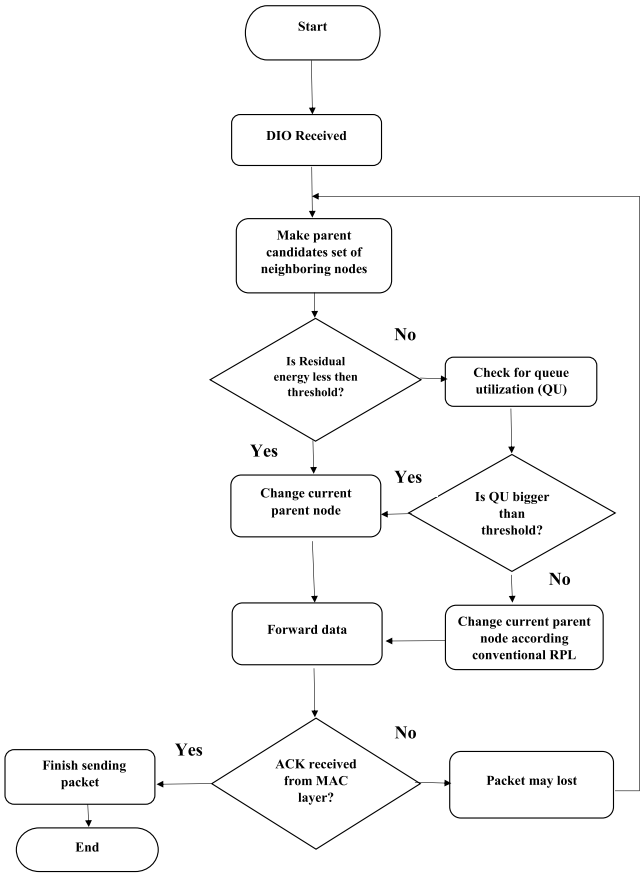

FIGURE 4. Process of the proposed scheme.

Step 4. In the first case, the residual energy of current parent node will be checked according Eq. (5). Current parent node will be switched to best alternative parent node, if the residual energy is less than a certain level/threshold as defined in Eq. (6).

Step 5. If the residual energy found within a threshold, then queue utilization of current parent node will be checked according Eq. (7).

Step 6. If queue utilization of current parent node is more than a certain level or threshold, then next preferred parent node will be selected according Eq. (9).

Step 7. Else current parent node will be changed as in conventional RPL protocol based on lower rank and lower ETX value.

Step 8. After parent node selection process, the data will be forwarded to preferred parent node.

Step 9. Receiving an acknowledgement packet form MAC layer means that the packet has successfully been received by the parent node.

Step 10. If no acknowledgment received from MAC layer, then packet may be lost and retransmission may be required. Therefore, the process will be repeated by going again to step 2.

For carrying information about Hop count, ETX, QU and Residual Energy, we exploited the Options field of conventional DIO packet as shown in Fig. 5. The different fields of different objects are described below [23].

1) NODE STATE ATTRIBUTE OBJECT

The Node State and Attribute (NSA) object is used to provide information on node characteristics such as congestion situation, CPU and memory. The NSA Routing Metric or Constraint type has been assigned value 1 by Internet Assigned Numbers Authority (IANA) [23].

The format of the NSA object body is shown in Fig. 5 and different fields are described below.

Res flags (8 bits): This is reserved field and must be set to zero on transmission and must be ignored on receipt.

Flags field (8 bits): The following two bits of the NSA object are currently defined:

'A' flag: This is data aggregation attribute. When set, this indicates that the node can act as a traffic aggregator for reducing the amount of traffic on the network.

'O' flag: O is a node workload used during path calculation. When set, this indicates that the node is overloaded and may not be able to process traffic. The unspecified flag fields must be set to zero on transmission and must be ignored on receipt. The Flags field of the NSA Routing Metric or Constraint object is managed by IANA. Unassigned bits are considered as reserved.

Optional TLVs: Type Length Value (TLV) is created by IANA and used to carry additional information about node characteristics. A Routing Metric or Constraint TLV is comprised of 1 byte for the type, 1 byte specifying the TLV length, and a value field. The TLV length field defines the length of the value field in bytes (from 0 to 255).

2) NODE ENERGY OBJECT

The Node Energy (NE) object is used to provide information related to node energy and may be used as a metric or as constraint. The NE object Type has been assigned value 2 by IANA. The NE object may contain additional TLVs.

The format of the NE object body is shown in Fig. 5 and different fields are described below.

Flags field (8 bits): The following flags are currently defined:

I (included): the 'I' bit is used when the path must only traverse mains-powered nodes. When set, this indicates that nodes of the type specified is included and must contain main powered nodes. When cleared, this indicates that nodes are battery operated.

T (node Type): The 2-bit field T indicating the node type. T=0 designates a mains-powered node, T=1 a battery-powered node, and T=2 a node powered by an energy scavenger.

E (Estimation): When the 'E' bit is set for a metric, the estimated percentage of remaining energy on the node is indicated in the E_E 8-bit field as shown in Fig. 5. When cleared, the estimated percentage of remaining energy is not provided. When the E bit is set, the E_E field defines a threshold for the inclusion or exclusion: if an inclusion, nodes

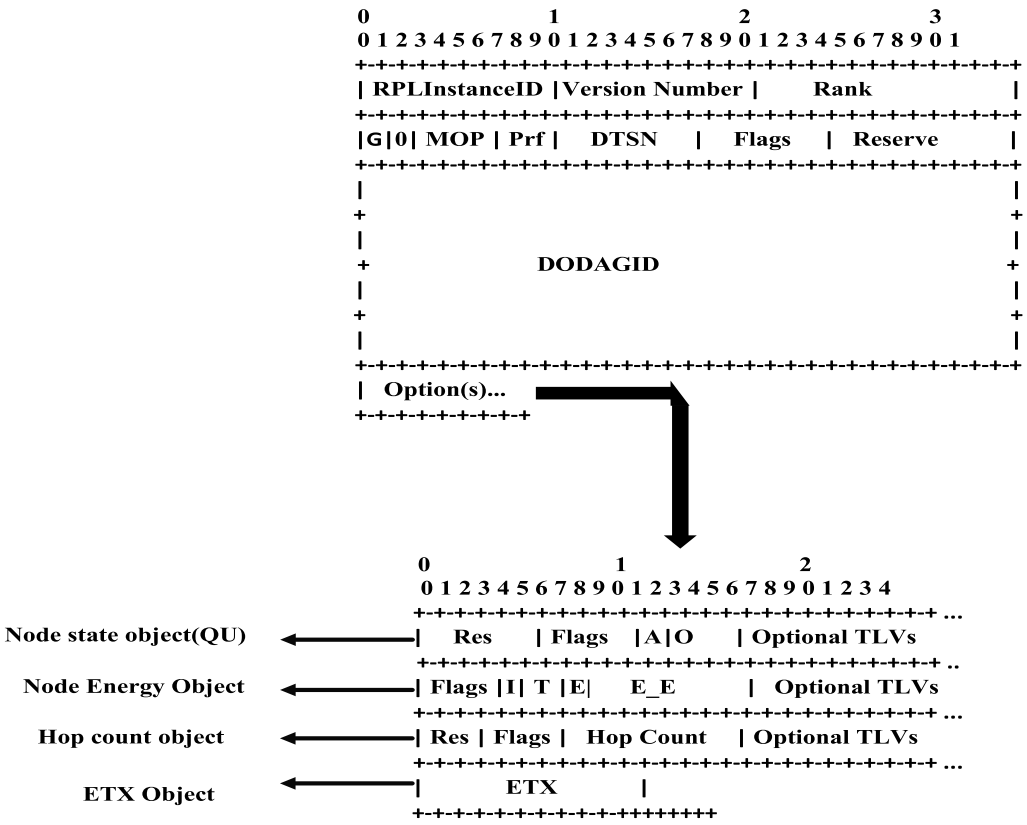

FIGURE 5. Amended RPL DIO Packet Format.

with values higher than the threshold are to be included; if an exclusion, nodes with values lower than the threshold are to be excluded.

E_E (Estimated-Energy): 8-bit unsigned integer field indicating an estimated percentage of remaining energy. The E_E field is only applicable when the 'E' flag is set, and it must be set to 0 when the 'E' flag is cleared.

3) HOP COUNT OBJECT

The Hop Count (HP) object is used to report the number of traversed nodes along the path. The HP object may also contain a set of TLVs used to convey various node characteristics. No TLV is currently defined. The HP routing metric object type has been assigned value 3 by IANA.

The format of the HP object body is shown in Fig. 5 and different fields are described below.

Res (4 bits): Reserved field must be set to zero on transmission and must be ignored on receipt.

Flags field (8 bits): No Flag is currently defined for HP.

Hop Count (8 bits): The HP object may be used as a constraint or a metric. When used as a constraint, the DAG root indicates the maximum number of hops that a path may traverse. When that number is reached, no other node can join that path. When used as a metric, each visited node simply increments the Hop Count field. Note that the first node along a path inserting a Hop Count metric object must set the Hop Count field value to 1 [23].

4) THE ETX RELIABILITY OBJECT

The ETX metric is the number of transmissions a node expects to make to a destination in order to successfully deliver a packet as explained in section II. Each ETX sub-object has a fixed length of 16 bits for encoding the ETX value as depicted in Fig. 5. The ETX object does not contain any additional TLVs and has been assigned value 7 by IANA.

IV. PERFORMANCE EVALUATIONS

A. SIMULATION ENVIRONMENT

The proposed scheme is evaluated by Cooja Simulator using the Contiki 3.0 operating system (OS) [24]. AMI networks are practically deployed as static multi-hop mesh network, that's why grid topology is used for performance evaluations. Many utility companies are using wireless communication technology. Our scheme and all related work of RPL are not designed for AMI networks only. It may be used for other application as well. Devices in the wireless environment can be mobile or fixed depending on the application and deployment. Therefore, we also simulate our scheme for random topology with mobile nodes. As shown in Fig. 6, random topology contained one server node acting as the root of the DODAG and client nodes. The number of client nodes varied from 20 to 100, with a step size of 20. The grid topology consisted of a DODAG root and 40 nodes that emulated Tmote sky sensors, each spaced 30 meters from the other. The sink node was located in front of the nodes, as shown in Fig. 7. To introduce

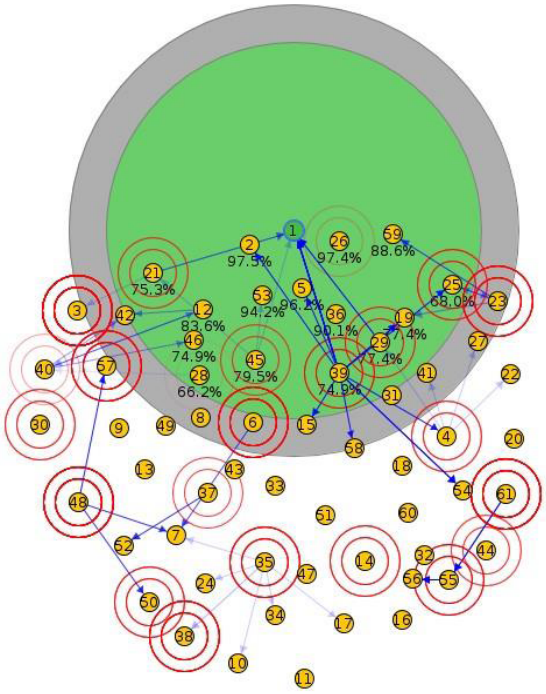

FIGURE 6. RPL random topology.

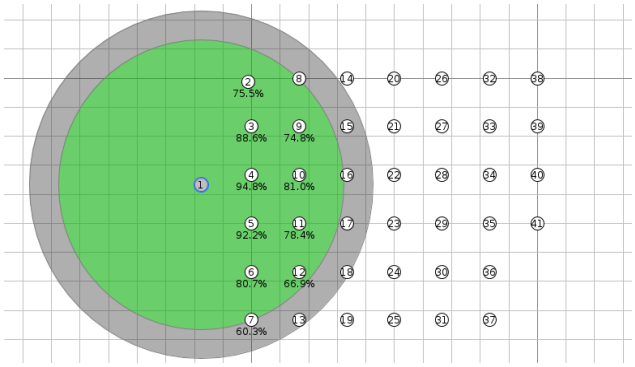

FIGURE 7. RPL grid topology.

lossiness into the wireless medium, we used the Cooja Unit Disk Graph Medium (UDGM) channel model, which applies lossiness with respect to the relative distances of nodes in the radio medium. The numbers in the figure shows the packet reception ratio (RX) in unit of percentage (%), indicating the lossiness of the wireless medium, meaning a nodes packet reception increases as the distance between the receiving node and the transmitting node decreases. RX means the rate of successful packet reception at the receiver. That means if the RX value is 50%, then 50% packets will be successfully received at the receiver. Transmission and interference ranges of 50 and 60 meters were used, respectively. The green areas in Fig. 6 and Fig. 7 represent the transmission range, and the gray circle shows the areas of interference. The green node labeled as 1İ is the sink node, and all other nodes are the client nodes that send packets to the border router. The nodes were distributed randomly non-uniformly in an area of 300 × 300 meters for random topology. We used desgin parameters α and β throughout our simulation. α is the weight given to QU and β is the weight given to residual energy E_{res}. α and β should be greater than 1 to have notable effect on the parent node selection. Otherwise, QU and E_{res} has smaller effect than hop count. We used Packet Send Interval of 2, 4, 6, 8, 12 and 16s. For the fair comparison, Both of protocols uses the beacon-enabled MAC protocol with Radio Duty Cycling (RDC) check rate. RDC check rate defines how often a node needs wake up to send or receive packets in oder to reduce power consumption. We used RDC check rate of 16 Hz which is the default value of contiki OS, and this value has been proven as an appropriate value throughout many evaluation studies [27], [28].

We calculated energy consumption using the power-trace outputs [25] including transmission time, listen time, CPU time, and LPM time. The energy consumed during the transmission, listening/receiving, CPU, and LPM states were 0.0017944 mJ, 0.00199 mJ, 0.00016 mJ, and 0.000004 mJ, respectively. To calculate energy consumed by sky motes, we used the current values of each state from the Tmote sky datasheet [26] as follows:

$$E_{cons}(mJ) = \frac{[T_{CPU} \times I_{CPU} + T_{TX} \times I_{TX} + T_{RX} \times I_{RX} + T_{LPM} \times I_{LPM}]}{RTIMER\_ARCH\_SECOND} \times 3V \quad (10)$$

where I_{CPU} (=1.8 mA), I_{TX} (=19.5 mA), I_{RX} (=21.8 mA) and I_{LPM} (=0.0545 mA) represent the currents consumed during the CPU run time T_{CPU}, the radio transmit run time T_{TX}, radio listen run time T_{RX} and low power mode run time T_{LPM} (all expressed in ticks), respectively. In addition, in Eq. (10), 3V is an initial battery voltage level and *RTIMER_ARCH_SECOND* represents the number of ticks per second (=32768/s). The residual energy can be defined as follows:

$$E_{res} = InitialEnergy - E_{cons} \quad (11)$$

The queue capacity was 10 packets and each packet size was 46 bytes. We chose γ of 0.5, meaning that the QU of a congested node is above 50%. The DIO interval minimum and doubling parameters were set to Contiki RPL defaults. We ran the simulation for two hours (7200s) for all simulated nodes. The simulation parameters and environments are shown in Table 2.

B. RESULTS AND DISCUSSION

The performance of the proposed scheme was compared to the other recently proposed scheme, which is ELPS [16]. Fig. 8 shows the impact of design parameters α and β on the performance of our proposed protocol ECRM. We note that PDR starts increasing for 0,1,2 value of α and β and then start decreasing after 2. The reason is that for the small values of α and β, the node chooses the short path and avoid congestion. For the large values of α and β, a node always

TABLE 2. Simulation parameters.

Parameter	Value
Simulator	Cooja Contiki 3.0
Radio Medium	UDGM
TX Ratio	100%
TX Range	50 meters
INT Range	60 meters
RX Ratio	20%, 40%, 60%, 80%, 100 %
Number of nodes	20, 40, 60, 80, 100
Energy Model	Energest
Area (m × m)	300 × 300
Initial Energy	10 J
EnergyConsumption(TX)	0.0017944 mJ
EnergyConsumption(RX)	0.00199 mJ
EnergyConsumption(CPU)	0.00016 mJ
EnergyConsumption(LPM)	0.000004 mJ
Simulation Time	2hours (7200s)
DIO Min	12
DIO Doubling	8
MAC	802.15.4 (beaconenabled)
RDC channel check rate	16 Hz
Total Packets sent (approx)	30000

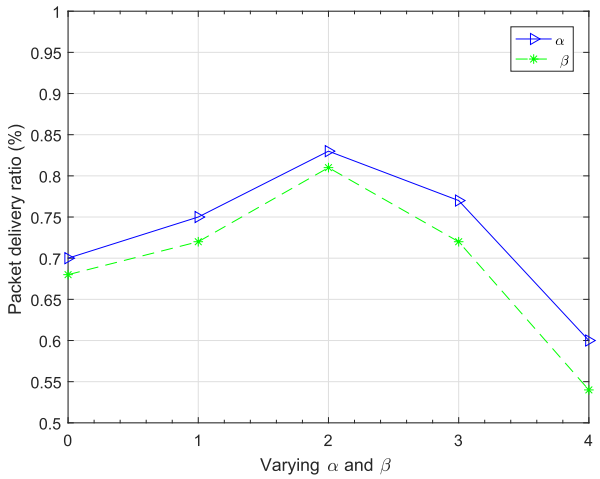

FIGURE 8. PDR as a function of varying α and β.

considers both of queue utilization and residual energy for selecting best-preferred parent node. Traffic congestion is easily avoided for a large value of α. The nodes which have low residual energies are easily avoided by using a large value of β. The impact of selecting larger value results in avoiding congested and energy constrained nodes. However, the longer path may be selected than the shortest path by ignoring hop count information of parent candidates. We note that these design parameters affect the performance of our protocol. Fig. 8 shows that Value 2 is an appropriate value for the performance of our protocol. Therefore, we used 2 for both of α and β. Through this value, the congestion and energy deficiency can be avoided by at most one hop count.

Average power consumption and PDR were evaluated as functions of number of RX levels and number of nodes.

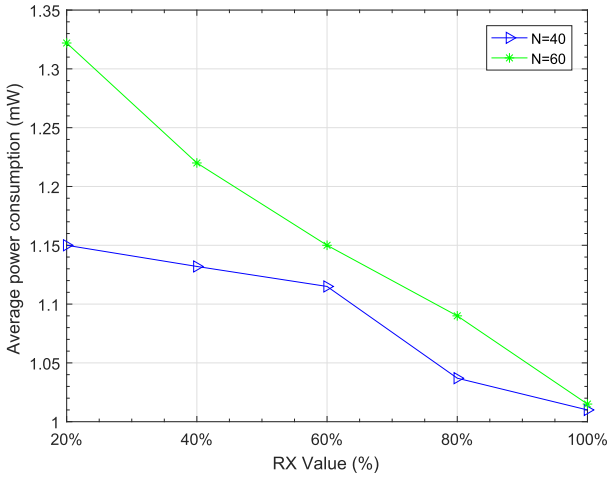

FIGURE 9. Average Power consumption as a function of the RX values with node density of 40 and 60.

In Fig. 9, average power consumptions of all nodes are evaluated as function of RX level. The average power consumption is higher at the lower value of RX level than at the higher value of RX level because the high value of RX level indicates the less lossiness in the network. This is because lossy environments require more retransmissions than lossless environments, and more power is consumed as a result. As we increased the RX level, the network became less lossy and required fewer retransmissions, which resulted in decreased power consumption. Furthermore, as shown in Fig. 9, the average power consumption for N = 60 is higher than that for N = 40. The reason is that power consumption is higher when the number of nodes is higher as compared to less number of nodes. More control messages sent in the network for the creation of DODAG. As a result, control traffic overhead increased in the network. Moreover, high-density nodes show more collisions in the network as compared to less number of nodes. In the low-density network, the packet loss is relatively small because of the fewer radio collisions.

In Fig. 10 and Fig. 11, in terms of average power consumption, the proposed scheme outperformed ELPS in both random and grid topology. In order to evaluate the performances over the various channel conditions, both topologies in Fig. 10 and Fig. 11 are evaluated in relatively bad channel condition (RX=40%) and good channel condition (RX=80%).

In both cases, our proposed scheme outperformed ELPS in terms of average power consumption. The reason is that as the number of nodes increases, the network traffic also increases; as a result, a greater number of nodes face energy deficiencies. The residual energies of many nodes become less than the threshold in Eq. (4), which creates energy holes. Once the nodes run out of energy, the network must trigger the local or global repair mechanism to reconfigure its topology. Configuration messages are broadcasted again to rebuild the network, which results in more power consumption. Unlike Grid topology, since mobile nodes in the random topology

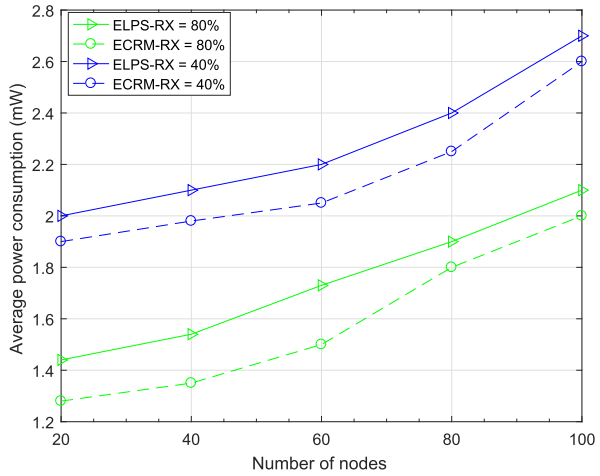

FIGURE 10. Average power consumption as a function of the number of nodes, using random topology.

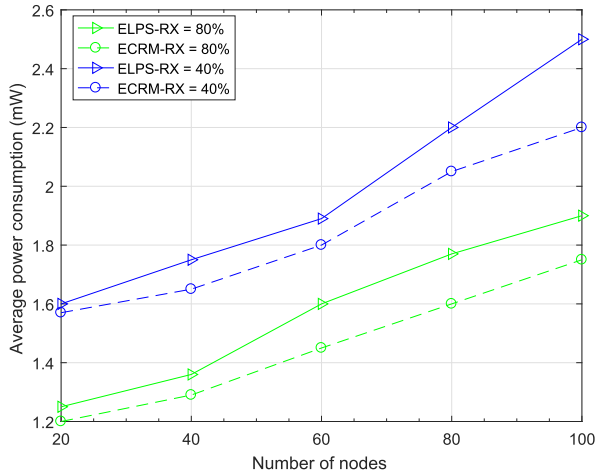

FIGURE 11. Average Power consumption as a function of the number of nodes using grid topology.

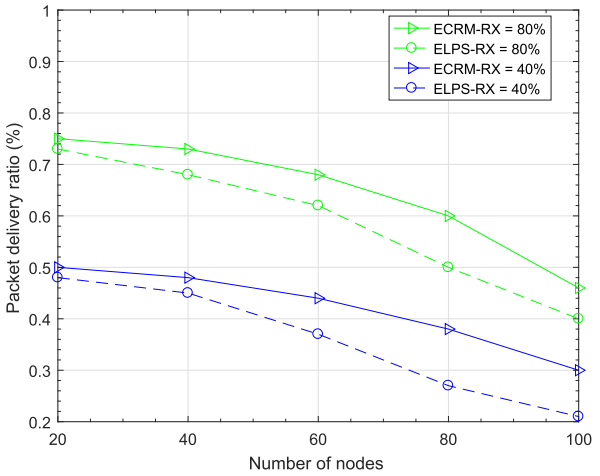

FIGURE 12. PDR as a function of the number of nodes, using random topology.

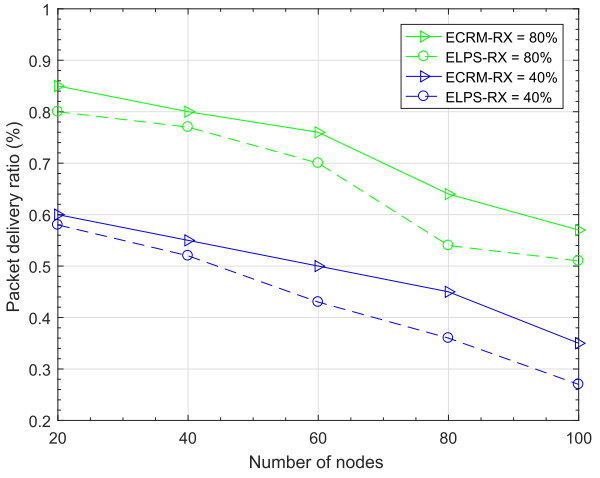

FIGURE 13. PDR as a function of the number of nodes, using grid topology.

moves around the network, the more power is relatively consumed comparing to the Grid topology.

Fig. 12 and Fig. 13 show that in networks with 20 nodes and 40 nodes, the PDRs of both schemes are likely the same across random and grid topologies for worst and best channel conditions. The reason for this is, in small networks, traffic is low and nodes do not face battery issues. As the network becomes larger, most of the nodes run out of energy. As a result, many packets are lost due to battery depletion. As soon as the energy level of current parent nodes decrease, the other candidate nodes become the strongest parent nodes, another node becomes optimal, thus requiring reconfigurations of the DODAG. These changes may create routing loops due to inconsistencies. However, in our proposed scheme, nodes will choose parent nodes that provide greater residual energy than the threshold, resulting in less packet loss at the parent node and fewer chances of DODAG reconfigurations and routing loops. In the worst channel condition the power consumption is higher than best channel condition. However, in both channel conditions our proposed scheme outperforms ELPS in terms of average power consumption and PDR.

In order to analyze the true effect and true importance of congestion aware sub-metric, we used various Send Intervals (traffic generation/traffic load). Send Interval is the frequency of application messages from client node to sink node. Resources consume very quickly, when the frequency of application messages is very fast. If we transmit packets after each 2 seconds, it result in increase of network traffic and radio collision. The queue become congested very quickly and high packet loss occurs as shown in Fig. 14.

Fig. 15 shows average power consumption as a function of varying Send Intervals. The more power is consumed when frequency of application messages is high. When we increase the Send Interval, the Energy Consumption decreases as shown in the Fig. 15. The Energy Consumption start decreasing in a linear way as the frequency of application messages decreased (Send Interval increases). We can decrease Energy Consumption as much as we can decrease frequency of application messages.

Fig. 16 shows PDR as a function of Send Interval. When we increase the Send Interval from 2s to 16s, the PDR

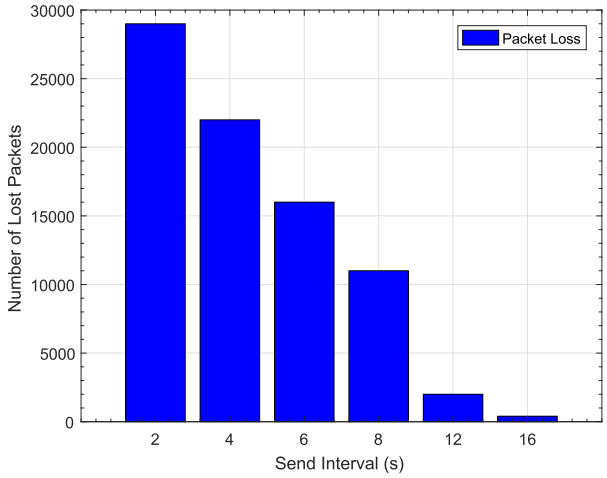

FIGURE 14. Number of Lost Packets as a function of Send Interval.

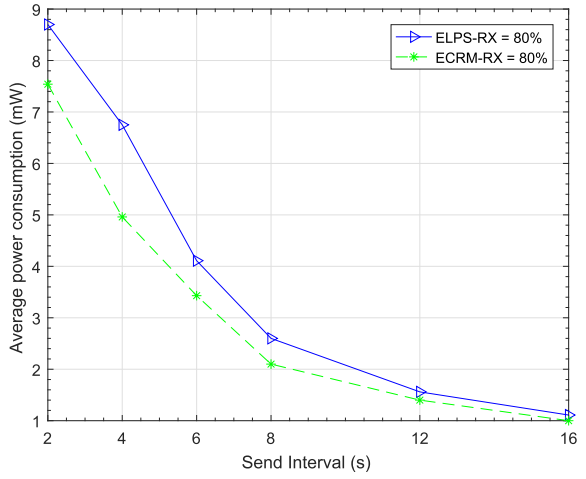

FIGURE 15. Average power consumption as a function of Send Interval.

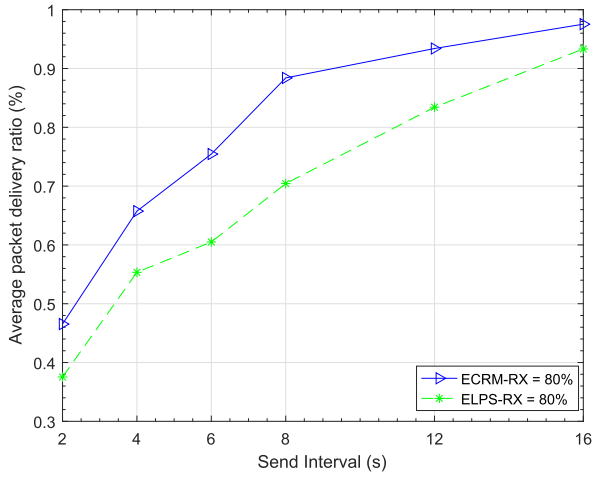

FIGURE 16. Average PDR as a function of Send Interval.

also increase for both protocols. More traffic load introduce congestion at buffers, radio collision and hence loss of packets. Fig. 15 and Fig. 16 reflects the true impact of congestion metric. Our proposed scheme ECRM outperforms ELPS [16] in terms of average power consumption and PDR for the different packet Send Intervals.

V. CONCLUSION

In this article, we proposed a dynamic parent node selection mechanism in RPL for smart metering in AMI networks, considering both residual energy and queue utilization. First, we studied the residual energy of the neighboring nodes to avoid routing loops and inconsistencies in the DODAG. Average power consumption and PDR is evaluated in worst and best channel conditions for the RX level 40% and 80% respectively. Second, we considered the queue utilization of the neighboring nodes to avoid network congestion. Minimum hop counts and unreliable links between the node and the root were also examined. We compared our scheme with the newly proposed ELPS. The simulation results show that our proposed scheme outperforms ELPS in terms of average power consumption and PDR in worst and best channel conditions.

REFERENCES

[1] C.-H. Lo and N. Ansari, "The progressive smart grid system from both power and communications aspects," *IEEE Commun. Surveys Tuts.*, vol. 14, no. 3, pp. 799–821, 3rd Quart., 2012.

[2] Z. Fan *et al.*, "Smart grid communications: Overview of research challenges, solutions, and standardization activities," *IEEE Commun. Surveys Tuts.*, vol. 15, no. 1, pp. 21–38, 1st Quart., 2013.

[3] Z. Yang, S. Ping, A. Aijaz, and A.-H. Aghvami, "A global optimization-based routing protocol for cognitive-radio-enabled smart grid AMI networks," *IEEE Syst. J.*, to be published.

[4] S. Spinsante, M. Pizzichini, M. Mencarelli, S. Squartini, and E. Gambi, "Evaluation of the wireless M-bus standard for future smart water grids," in *Proc. 9th Int. Wireless Commun. Mobile Comput. Conf. (IWCMC)*, Jul. 2013, pp. 1382–1387.

[5] R. R. Mohassel, A. Fung, F. Mohammadi, and K. Raahemifar, "A survey on advanced metering infrastructure," *Int. J. Elect. Power Energy Syst.*, vol. 63, pp. 473–484, Dec. 2014.

[6] E. Ancillotti, R. Bruno, and M. Conti, "The role of the RPL routing protocol for smart grid communications," *IEEE Commun. Mag.*, vol. 51, no. 1, pp. 75–83, Jan. 2013.

[7] *Applicability Statement for the Routing Protocol for Low-Power and Lossy Networks (RPL) in Advanced Metering Infrastructure (AMI) Networks*, document RFC 8036, Jan. 2017.

[8] M. Qasem *et al.*, *Load Balancing Objective Function in RPL Draftqasem-Roll-RPL-Load Balancing-00 Draft*, document, Feb. 2017. [Online]. Available: https://datatracker.ietf.org/doc/html/draft-qasem-roll-rpl-load-balancing-00

[9] T. Winter *et al.*, *RPL: IPv6 Routing Protocol for Low-Power and Lossy Networks, Internet Engineering Task Force (IETF)*, document RFC 6550, Mar. 2012.

[10] T. Watteyne, A. Molinaro, M. G. Richichi, and M. Dohler, "From MANET to IETF roll standardization: A paradigm shift in wsn routing protocols," *IEEE Commun. Surveys Tuts.*, vol. 13, no. 4, pp. 688–707, 4th Quart., 2011.

[11] J. Lloret, J. Tomas, A. Canovas, and L. Parra, "An integrated IoT architecture for smart metering," *IEEE Commun. Mag.* vol. 54, no. 12, pp. 50–57, Dec. 2016.

[12] V. C. Gungor *et al.*, "A survey on smart grid potential applications and communication requirements," *IEEE Trans. Ind. Informat.*, vol. 9, no. 1, pp. 28–42, Feb. 2013.

[13] T. Winter, P. Thubert, A. R. Corporation, and R. Kelsey, *RPL: IPv6 Routing Protocol for Low Power and Lossy Networks*, document RFC 6550, Mar. 2012.

[14] A. Aijaz, S. Ping, M. R. Akhavan, and A. Aghvami, "CRB-MAC: A receiver-based MAC protocol for cognitive radio equipped smart grid sensor networks," *IEEE Sensors J.* vol. 14, no. 12, pp. 4325–4333, Dec. 2014.

[15] H.-S. Kim, H. Kim, J. Paek, and S. Bahk, "Load balancing under heavy traffic in RPL routing protocol for low power and lossy networks," *IEEE Trans. Mobile Comput.*, vol. 16, no. 4, pp. 964–979, Apr. 2016.
[16] M. Nassiri, M. Boujari, and S. V. Azhari, "Energy-aware and load-balanced parent selection in RPL routing for wireless sensor networks," *Int. J. Wireless Mobile Comput.*, vol. 9, no. 3, pp. 231–239, 2015.
[17] O. Gnawali *et al.*, *The Minimum Rank With Hysteresis Objective Function*, document RFC 6719, Sep. 2012.
[18] P. Thubert *et al.*, *Objective Function Zero for the Routing Protocol for Low-Power and Lossy Networks (RPL)*, document RFC 6552, Mar. 2012.
[19] D. S. J. De Couto, D. Aguayo, J. Bicket, and R. Morris, "A high-throughput path metric for multi-hop wireless routing," in *Proc. 9th Annu. Int. Conf. Mobile Comput. Netw. (MobiCom)*, Sep. 2005, pp. 419–434.
[20] O. Gaddour, A. Koubaa, N. Baccour, and M. Abid, "OF-FL: QoS-aware fuzzy logic objective function for the RPL routing protocol," in *Proc. 12th Int. Symp. Modeling Optim. Mobile Ad-Hoc Wireless Netw.*, May 2014, pp. 365–372.
[21] M. Ha, K. Kwon, P.-Y. Kong, and D. Kim, "Dynamic and distributed load balancing scheme in multi-gateway based 6LoWPAN," in *Proc. IEEE/ACM iThings*, Sep. 2014, pp. 87–94.
[22] X. Liu, J. Guo, G. Bhatti, P. Orlik, and K. Parsons, "Load balanced routing for low power and lossy networks," in *Proc. IEEE Wireless Commun. Netw. Conf.*, Apr. 2013, pp. 2238–2243.
[23] J. P. Vasseur, M. Kim, and K. Pister, *Routing Metrics Used for Path Calculation in Low-Power and Lossy Networks*, document RFC 6551, Mar. 2012.
[24] A. Dunkels, B. Gronvall, and T. Voigt, "Contiki—A lightweight and flexible operating system for tiny networked sensors," in *Proc. 29th Annu. IEEE Int. Conf. Local Comput. Netw.*, Nov. 2004, pp. 455–462.
[25] A. Dunkels, J. Eriksson, N. Finne, and N. Tsiftes, "Powertrace: Network-level power profiling for low-power wireless networks," SICS, Kista, Sweden, Tech. Rep. T2011:05, Mar. 2011.
[26] *Tmote Sky: Ultra Low Power IEEE 802.15.4 Compliant Wireless Sensor Module*. Moteiv Corporation, San Francisco, CA, USA, 2006.
[27] M. Michel and B. Quoitin. (Apr. 2014). "Technical report: ContikiMAC vs X-MAC performance analysis." [Online]. Available: https://arxiv.org/abs/1404.3589
[28] A. Dunkels, "The ContikiMAC radio duty cycling protocol," Swedish Inst. Comput. Sci., Stockholm, Sweden, Tech. Rep. T2011:13, 2011.

REHMAT ULLAH received the B.S. degree in computer science from the COMSATS Institute of Information Technology, Attock, Pakistan, in 2013, and the M.S. degree in computer science from the COMSATS Institute of Information Technology, Islamabad, Pakistan, in 2016. He is currently pursuing the Ph.D. degree with the Broadband Convergence Networks Laboratory with the Department of Electronics and Computer Engineering, Hongik University, South Korea. His major interests are in the field of wireless CCNs/NDNs, IoT, 5G, and Edge computing.

YASIR FAHEEM received the B.S. degree in computer science from NUCES-FAST, Pakistan, in 2006, the M.S. Research degree with specialization in networks and distributed systems from Université Nice Sophia Antipolis, France, in 2008, and the Ph.D. degree from Networks and Information Technologies, Université Paris Nord, France, in 2012. He is currently an Assistant Professor with the Department of Computer Science, COMSATS Institute of Information Technology, Pakistan. His current research interests are in cognitive radio networks, wireless sensor networks, opportunistic networks, cloud computing and Internet of Things. He has served as a TPC Member of the IEEE ICC, the IEEE Globecom, and various other conferences. He serves as a Reviewer of the IEEE *Communications Magazine*, the *Elsevier Journal of Network and Computer Applications*, and various key conferences.

BYUNG-SEO KIM (M'02) received the B.S. degree in electrical engineering from In-Ha University, In-Chon, South Korea, in 1998, and the M.S. and Ph.D. degrees in electrical and computer engineering from the University of Florida in 2001 and 2004, respectively. His Ph.D. study was supervised by Dr. Y. Fang. From 1997 to 1999, he was a Computer Integrated Manufacturing Engineer with the Advanced Technology Research and Development, Motorola Korea Ltd., PaJu, South Korea. From 2005 to 2007, he was a Senior Software Engineer with Networks and Enterprises, Motorola Inc., Schaumburg, IL, USA. His research focuses in Motorola Inc., were designing protocol and network architecture of wireless broadband mission critical communications. He is currently an Associate Professor with the Department of Computer and Information Communication Engineering, Hongik University, South Korea. His work has appeared in around 141 publications and 22 patents. His research interests include the design and development of efficient wireless/wired networks, including link-adaptable/cross-layer-based protocols, multi-protocol structures, wireless CCNs/NDNs, mobile edge computing, physical layer design for broadband PLC, and resource allocation algorithms for wireless networks. He was served as a member of the Sejong-city Construction Review Committee and the Ansan-city Design Advisory Board and a TPC Member of the IEEE VTC 2014-Spring, the EAI FUTURE2016, and ICGHIC 2016 and 2017 conferences. He was the Chairman of the Department from 2012 to 2014. He served as a Guest Editor of the *Journal of the Institute of Electrics and Information Engineers*. He also served as a Guest Editors of special issues of *International Journal of Distributed Sensor Networks* and IEEE Access.